

Supplementary Information

Table of Content

1. General remarks
2. Rule based model of the insulin receptor binding
3. Rule based model of the IGF1 receptor binding
4. Reaction scheme for the insulin/IGF1 receptor binding
5. Modelling receptor recycling
6. Modelling of the competition experiment
7. Modelling of the ligand dependence of the dissociation rate
8. Fitting of the model to the experimental data
9. Supplementary Discussion
10. Supplementary figures

1. General remarks

In order to avoid unnecessarily complex designations for the receptor intermediaries and their corresponding concentrations, the same designations will be used, meaning that if *e.g.* the designation r_0 is used in a reaction scheme, it should be understood as a designation of a compound, whereas in equations and formulas the same designation r_0 should be understood as the concentration of this compound.

2. Rule based model of the insulin receptor binding

The assumptions and definitions of the various terms required for mathematical modelling are described in the main text of the article. These assumptions can be represented as a set of rules

(see Fig. S1), which can be used for the computer-assisted generation of the interaction network, but can also be quite helpful for the traditional way of modelling with the help of reaction schemes.

Rules 1 and 2 describe binding of insulin to the inactive conformations of the receptor. The insulin molecule can bind to any of the four sites, but only one molecule can bind to the same crosslink (see the main text for explanation). Application of these two rules to the un-bound form of the receptor leads to formation of 8 inactive intermediaries (see Fig. S2).

Rules 3 and 4 describe activation (crosslinking) of the receptor. Application of these rules to the above 8 inactive intermediaries produces 6 crosslinked (active) intermediaries with either one or zero insulin molecules bound to the other crosslink (see Fig. S2).

Rules 5 and 6 describe binding of a third insulin molecule to the activated conformation of the insulin receptor. Rule 7 describes dimerization of insulin with a dissociation constant (K_d) of approximately 7 μM . Binding of the insulin dimer to the receptor's site 2 is described by rule 8. Application of rules 5-8 leads to formation of 4 crosslinked (activated) intermediaries with three insulin molecules bound (see Fig. S2).

3. Rule based model of the IGF1 receptor binding

As justified in the main text, only the first four rules are applicable to the IGF1 receptor.

4. Reaction schemes for the insulin/IGF1 receptor binding

Each of the intermediaries shown in Fig. S2 can be converted into some other intermediaries if the rules allow. Let us consider for example the r_{1x2} intermediary. It can be converted into r_2 (rule 4), r_1 (rule 3), r_{1x24d} (rule 8), r_{1x24} (rule 2) and r_{1x23} (rule 1). No other reactions are possible for the r_{1x2} intermediary. This can be verified by going through all other intermediaries and checking if a rule exists that would allow conversion of r_{1x2} into them. The above 5 reactions are shown in Fig. S3 (k_4 and k_8 are the association and dissociation rate constants, respectively, for insulin dimerization) as

a reaction scheme number 6. For each of the other 18 intermediaries, a similar reaction scheme can be created. All of these reaction schemes are shown in Fig. S3.

However, for modelling the ligand dependence of the dissociation rate, two types of ligands should be considered: "hot" and "cold" (see the main text for explanation). Thus, each insulin molecule in the intermediaries shown in Fig. S2 can be either hot or cold, which creates 77 distinct intermediaries. The process described above can be applied to these 77 intermediaries, but if one imposes the initial conditions of the experimental set-up (see the main text), some of the intermediaries will never be formed.

Normally, the insulin receptor is incubated with 20 pM hot insulin for two hours. Hot insulin is then removed, and the complex of hot insulin with the insulin receptor is allowed to dissociate in the presence of cold insulin for a certain period of time. One can intuitively see that binding of 20 pM insulin would lead to formation of mostly r_{1x2} and r_{3x4} intermediaries (subsequent calculations show that it is about 99%), which means that it is sufficient to consider the dissociation of only hot r_{1x2} (r_{3x4} is indistinguishable from r_{1x2}). Since the concentration of hot insulin is zero, its dissociation becomes irreversible, and only intermediaries that arise due to binding/dissociation of cold insulin and/or dissociation of hot insulin should be considered. For the mixed intermediaries (bound to hot and cold insulin), the same designations as shown in Fig. S2 will be used, and the hot insulin molecule will be indicated by "h" to the right of the corresponding index. r_{1x2} with the hot insulin is thus designated as r_{1x2h} . r_{1x2h} can dissociate into r_{1h} and r_{2h} , and bind up to two cold insulin molecules (as well as the insulin dimer), leading to r_{1x2h4} , r_{1x2h3} , r_{1x2h34} and r_{1x2h4d} (Fig. S4). r_{1h} and r_{2h} can dissociate into r_0 , which can bind to cold insulin, leading to formation of 19 cold intermediaries described above (Fig. S2). r_{1h} and r_{2h} can also bind to a cold insulin molecule, leading to r_{1h3} , r_{1h4} , r_{2h3} and r_{2h4} , which can become crosslinked, leading to r_{1h3x4} , r_{2h3x4} , which in turn can bind to a second cold insulin molecule, leading to r_{1h23x4} , r_{12h3x4} and r_{2hd3x4} (Fig. S4). In all, 35 intermediaries are, thus, required for modelling (instead of 77). The reaction scheme for the 16

new (see Fig. S4) intermediaries (containing hot insulin) is shown in Fig. S5, which can be created using the above described method with the use of rules shown in Fig. S1.

The reaction schemes for the IGF1 receptor can be created in a similar way.

5. Modelling insulin receptor recycling

Since insulin receptor recycling is very slow at 15 °C, we used a minimal recycling model, in which only the fastest processes are taken into account. The activated intermediaries (those which are crosslinked) are assumed to be endocytosed with a rate constant, k_{end} , whereas the much slower endocytosis of the inactive intermediaries is considered to be negligible. The endocytosed receptor-ligand intermediaries are assumed to dissociate instantly because of the reduced pH in the endosomes and exocytosed back to the membrane with a rate constant k_{exo} , while the dissociated insulin is expelled out of the cell with the same rate constant. Ligand and receptor degradation is not considered because at 15 °C degradation does not seem to happen or is extremely slow.

6. Modelling of the competition experiment

Binding of insulin to the insulin receptor leads to formation of 19 insulin receptor intermediaries shown in Fig. S2. The reaction scheme for each of these intermediaries is shown in Fig. S3 (k_4 and k_8 are the association and dissociation rate constants, respectively, for insulin dimerization). The activated intermediaries (r_{1x2} , r_{3x4} , r_{1x23} , r_{1x24} , r_{13x4} , r_{23x4} , r_{1x234} , r_{123x4} , r_{2d3x4} and r_{1x24d}) are also subject to endocytosis with an endocytosis rate constant, k_{end} . Upon endocytosis, these intermediaries are assumed to dissociate instantly into cytoplasmic receptor (r_{0cyt}) and cytoplasmic insulin (i_{end}), which are then expelled from the cell with the exocytosis rate constant, k_{exo} . Combining the reaction scheme from Fig. S3 with the receptor recycling, one can obtain a system of ordinary differential equations, shown in Fig. S6, describing concentrations of the receptor intermediaries as functions of time. Let us consider, for example, how equation number 1 (shown in Fig. S6) was created. This equation describes formation of the r_0 intermediary on the surface of the

cells from r_1, r_2, r_3, r_4 (which are also on the surface of the cells) (see Fig. S3) and $r_{0\text{cyt}}$ (which is cytoplasmic r_0). Using the law of mass action, one obtains that the rate of r_0 formation (r_0') is equal to:

$$\begin{aligned}
& - a_1 \times r_0 \times i_m \text{ (which is the rate of } r_1 \text{ formation from } r_0 \text{ with a minus sign)} \\
& + d_1 \times r_1 \text{ (rate of } r_0 \text{ formation from } r_1) \\
& - a_2 \times r_0 \times i_m \text{ (rate of } r_4 \text{ formation from } r_0 \text{ with a minus sign)} \\
& + d_2 \times r_4 \text{ (rate of } r_0 \text{ formation from } r_4) \\
& - a_1 \times r_0 \times i_m \text{ (rate of } r_3 \text{ formation from } r_0 \text{ with a minus sign)} \\
& + d_1 \times r_3 \text{ (rate of } r_0 \text{ formation from } r_3) \\
& - a_2 \times r_0 \times i_m \text{ (rate of } r_2 \text{ formation from } r_0 \text{ with a minus sign)} \\
& + d_2 \times r_2 \text{ (rate of } r_0 \text{ formation from } r_2) \\
& + k_{\text{ex}} \times r_{0\text{cyt}} \text{ (rate of exocytosis of the cytoplasmic } r_0 \text{ to the surface),}
\end{aligned}$$

where i_m stands for the concentration of the monomeric insulin.

For every individual reaction scheme shown in Fig. S3, using the same method as in the example above, one obtains a corresponding differential equation. All of these equations are shown in Fig. S6.

It is assumed that insulin is in excess to the receptor, and the concentrations of the monomeric (i_m) and dimeric (i_d) insulin can be calculated from the total concentration of insulin (i_{tot}) in the following way:

$$i_d = (4 \cdot i_{\text{tot}} + KD - \sqrt{KD^2 + 8 \cdot i_{\text{tot}} \cdot KD}) / 8; \quad i_m = i_{\text{tot}} - 2 \cdot i_d, \quad \text{where } KD \text{ stands for the dissociation constant of the insulin dimerization (7 } \mu\text{M)}.$$

The system was solved by numerical integration for the required period of time (using Mathematica 5) with the following initial conditions: $r_0(0)=1, i_{\text{end}}(0)=0, r_x(0)=0$ ('x' stands for any index except for '0'). The total amount of insulin contained by cells after a certain period of time (bound to the receptor and endocytosed) was calculated with the following expression:

$$i_{\text{end}}+r_1+r_2+r_3+r_4+2r_{13}+2r_{14}+2r_{23}+2r_{24}+r_{1x2}+r_{3x4}+2r_{1x23}+2r_{1x24}+2r_{13x4}+2r_{23x4}+3r_{1x234}+3r_{123x4}+3r_{2d3x4}+3r_{1x24d}$$

7. Modelling of the ligand dependence of the dissociation rate

Interaction of r_{1x2h} with cold insulin in the absence of hot insulin leads to 16 intermediaries containing hot insulin (see Fig. S4) as well as to 19 intermediaries containing only cold insulin (see Fig. S2). The reaction scheme for the 16 hot intermediaries is shown in Fig. S5, which in combination with the reaction scheme from Fig. S3 (for the 19 cold intermediaries) makes a complete reaction scheme for description of the r_{1x2h} dissociation. As can be seen from Fig. S5, reactions number 21, 22, 27, 28, 29, 30, 31, 32, 33, 34 and 35 lead to cold intermediaries – r_0 , r_0 , r_4 , r_4 , r_3 , r_3 , r_{3x4} , r_{3x4} , r_{23x4} , r_{13x4} and r_{3x4} , respectively, which requires the corresponding modifications of the reactions number 1, 4, 5, 11, 14 and 15 from Fig. S3 (describing formation of these cold intermediaries from the hot intermediaries) in the r_{1x2h} dissociation reaction scheme. Combining this scheme with the receptor recycling (described above), one can obtain a system of ordinary differential equations describing r_{1x2h} dissociation in the presence of cold insulin, shown in Fig. S7.

Modelling preincubation of cells with tracer insulin. The binding of 24 pM tracer (hot insulin) for 2 hours was done as described in 'Modelling of the competition experiment', and the concentrations of r_0 , $r_{0\text{cyt}}$, r_{1x2} , r_{3x4} , r_1 , r_2 , r_3 , r_4 and i_{end} were determined after association of tracer for 2 hours.

Modelling r_{1x2h} dissociation in the presence of cold insulin. The system of ordinary differential equations shown in Fig. S7 was solved numerically for the required period of time with the following initial conditions: $r_0(0)=r_0^{\text{pre}}$, $r_{0\text{cyt}}(0)=r_{0\text{cyt}}^{\text{pre}}$, $r_{1x2h}(0)=r_{1x2}^{\text{pre}}+r_{3x4}^{\text{pre}}$, $r_{1h}(0)=r_1^{\text{pre}}+r_3^{\text{pre}}$, $r_{2h}(0)=r_2^{\text{pre}}+r_4^{\text{pre}}$, $i_{\text{end}}(0)=i_{\text{end}}^{\text{pre}}$, the concentrations of all other intermediaries were set to 0 (the subscript 'pre' means that the concentration corresponds to that calculated after preincubation with the 24 pM tracer for 2 hours). The total amount of hot insulin remaining in cells (bound and

endocytosed) after incubation of cells with cold insulin for a certain period of time was calculated with the following expression:

$$r_{1x2h} + r_{1h} + r_{2h} + r_{1x2h3} + r_{1x2h4} + r_{1x2h34} + r_{1h4} + r_{2h4} + r_{2h3} + r_{1h3} + r_{1h3x4} + r_{2h3x4} + r_{1h23x4} + r_{12h3x4} + r_{1x2h4d} + r_{2hd3x4} + i_{end}$$

8. Fitting of the model to the experimental data

Given a set of parameters, one can simulate (by solving numerically the corresponding differential equations) the above described experimental data. The goodness of fit between the experimental (x_i) and simulated (y_i) data points can be evaluated with a score function equal to

$$\frac{1}{N} \sum_{i=1}^N \frac{(x_i - y_i)^2}{sd_i^2},$$

where N is the number of data points and sd_i is the standard deviation of the corresponding experimental data point. To search for the parameters giving the best fit, the score function was minimized using a genetic algorithm (with random initial values of all of the parameters) in combination with gradient minimization. The starting value for the a_1 and a_2 parameters were 10^{x1} and 10^{x2} M s^{-1} , where $x1$ and $x2$ were randomly selected from 2 to 6; for d_1 and d_2 – 10^{x3} and 10^{x4} s^{-1} , where $x3$ and $x4$ were randomly selected from -5 to -1; for k_{cr} – 10^{x5} s^{-1} , where $x5$ was randomly selected from -2 to 2; for k_{end} and k_{exo} – 3.6×10^{x6} and $3.6 \times 10^{x7} \%$ per hour, where $x6$ and $x7$ were randomly selected from -2 to 2.

9. Supplementary Discussion

The crosslinking constant used in the model has a clear physical interpretation: its reciprocal is equal to the average time it takes for the insulin receptor to perform a spontaneous conformational change from the inactive state to the active, which is approximately 3 s. It is interesting to compare this value to the average time period it would take for the receptor subunits to perform the crosslinking by diffusion alone (assuming that the activation energy is zero, and that the receptor subunits freely diffuse within a certain distance range). Using a $0.1 \text{ } \mu\text{m}^2/\text{s}$ value for the diffusion

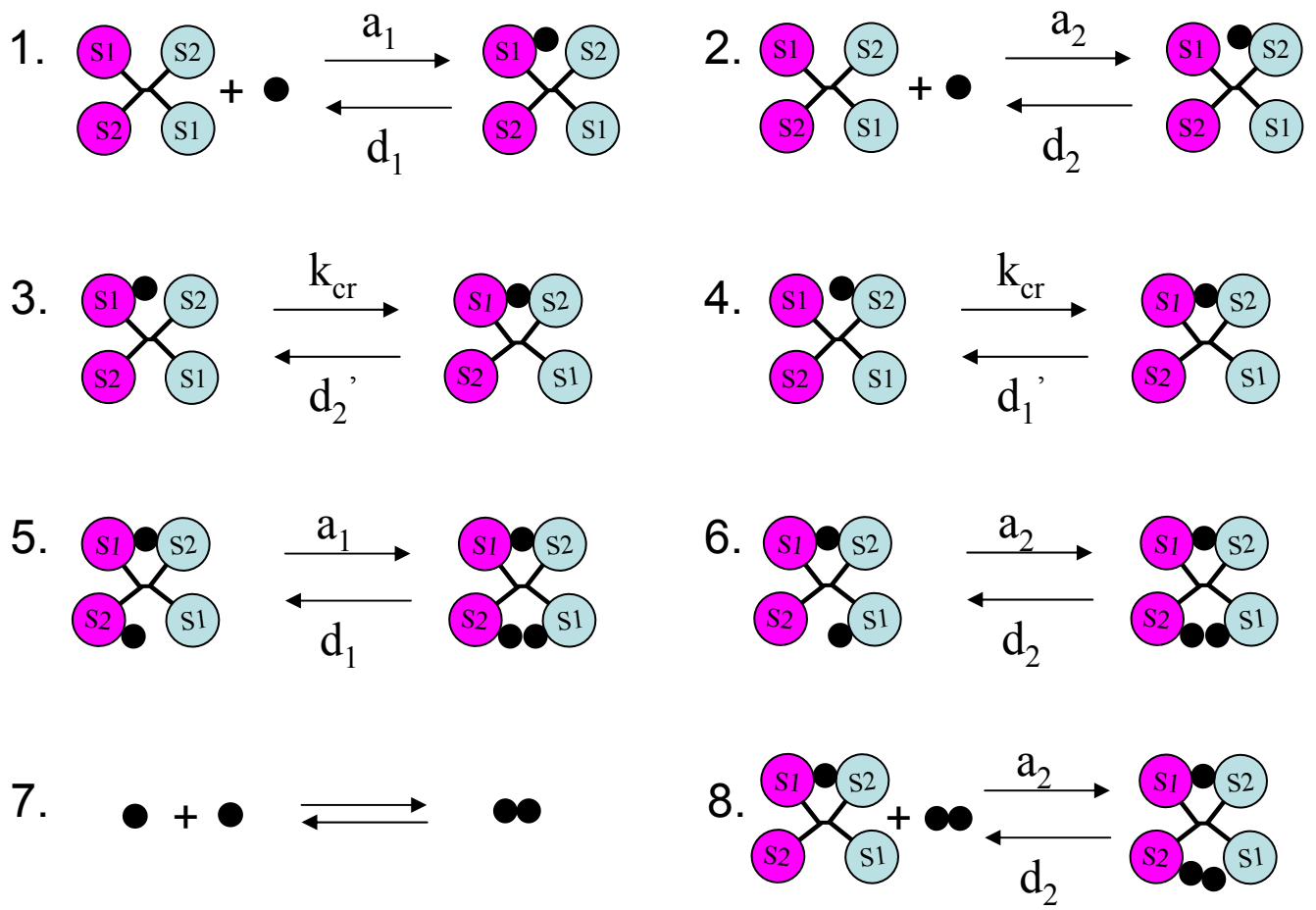
coefficient and a 4 nm distance range (which is twice the size of insulin), this time period can be roughly estimated as 0.2 ms. Thus, the presented model indicates that the crosslinking reaction of the insulin receptor is much slower than what one would expect from free diffusion of the receptor subunits. One reason is, obviously, that the activation energy is not zero, but another reason is that the conformational change is coupled with some movement of the receptor transmembrane subunits in the membrane, which is also expected to contribute to slowing down of the crosslinking reaction. Thus, a decrease in the membrane rigidity is expected to increase the value of the crosslinking constant, and the complete removal of the membrane (as in a soluble receptor) is expected to increase it even further. This increase in the crosslinking constant is predicted to increase the receptor affinity (see Fig. S8), which is in agreement with observations that soluble insulin receptor has much higher affinity (0.02 nM Kd) (Schäffer, 1994; see the references in the main text). It should also be noted that variation of the membrane composition due to differential expression of membrane proteins (and possibly differential lipid composition) by various cell types may lead to variation of the crosslinking constant, which could be the reason for the fact that the insulin receptor has different apparent affinities in different cells. As can be seen from Fig. S8, by varying the crosslinking constant from 10 times greater to 10 times smaller than the average value of 0.33 s^{-1} (and keeping the other parameters the same), the apparent Kd varies from 0.019 to 1.8 nM, which represents the range of the experimentally determined receptor affinities under various conditions.

Based on the known values of the parameters, it is possible to identify the dissociation routes that contribute most to this effect. The dissociation route in the absence of cold insulin is shown in Fig. S9 with red lines. It is easy to calculate from the known rate constants (see Fig. S9) that the steady state level of r_{1h} is approximately 3.3 % (or d_2/k_{cr} 100%) of the total receptor bound to hot insulin. Since r_{1h} dissociates with a rate constant d_1 , the apparent dissociate rate constant of hot insulin in the absence of cold insulin is approximately 3.3 % of d_1 (or $\frac{d_1 \cdot d_2}{k_{cr}}$),

which is equal to $1.2 \times 10^{-4} \text{ s}^{-1}$ (in good agreement with an experimentally determined apparent dissociation rate constant of $1.4 \times 10^{-4} \text{ s}^{-1}$, estimated from Fig. 5C of the main text). If the concentration of cold insulin is around 100 nM, then site 3 of r_{1x2h} will be very quickly saturated with cold insulin (Kd of 6.3 nM), but the occupancy of site 4 (Kd of 400 nM) will be very low. Thus, the route shown by black solid lines in Fig. S9 will be the major route of dissociation when the concentration of cold insulin is around 100 nM. The r_{1x2h3} intermediary will be converted into r_{1h3x4} (and vice versa) via a transiently existing r_{1h3} intermediary (Fig. S9). The steady state levels of these intermediaries will be approximately 49.2 % for r_{1x2h3} and r_{1h3x4} , and 1.7 % for r_{1h3} of the total receptor bound to insulin. Since the hot insulin molecule can dissociate from r_{1h3x4} with a rate constant d_1 (Fig. S9), the apparent dissociation rate constant of hot insulin will be approximately 49.2 % of d_1 (or for all practical purposes, $0.5 d_1$), which is equal to $1.53 \times 10^{-3} \text{ s}^{-1}$ (in good agreement with an experimentally determined apparent dissociation rate constant of $1.34 \times 10^{-3} \text{ s}^{-1}$, estimated from Fig. 5C of the main text). At insulin concentrations of more than $1 \mu\text{M}$, there will be substantial occupancy of site 4 of the r_{1x2h} intermediary (in addition to site 3), leading to formation of r_{1x2h34} (see the path indicated by the black dashed lines in Fig. S9), which contributes to the deceleration of the insulin receptor dissociation, because hot insulin cannot dissociate from this intermediary. Thus, the insulin receptor dissociation routes shown in Fig. S9 give a good overview of the insulin receptor dissociation and a reasonable approximation under special conditions such as no cold insulin, 100 nM cold insulin (fastest dissociation) and infinite cold insulin concentration (no dissociation). However, for the intermediate insulin concentrations, the complete network involving all 35 intermediaries (shown in Fig. S2 and S4) should be used.

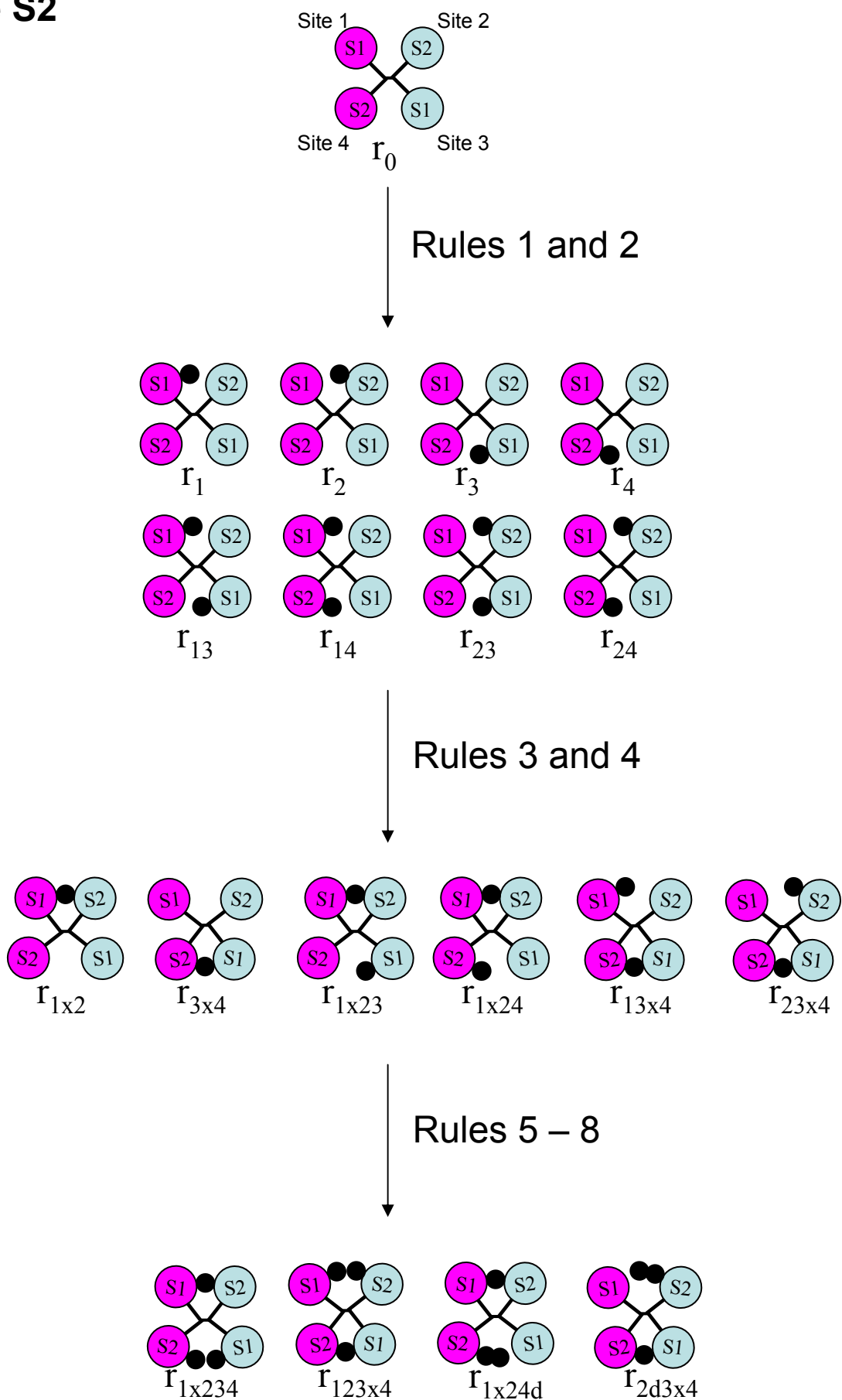
10. Supplementary figures

Figure S1



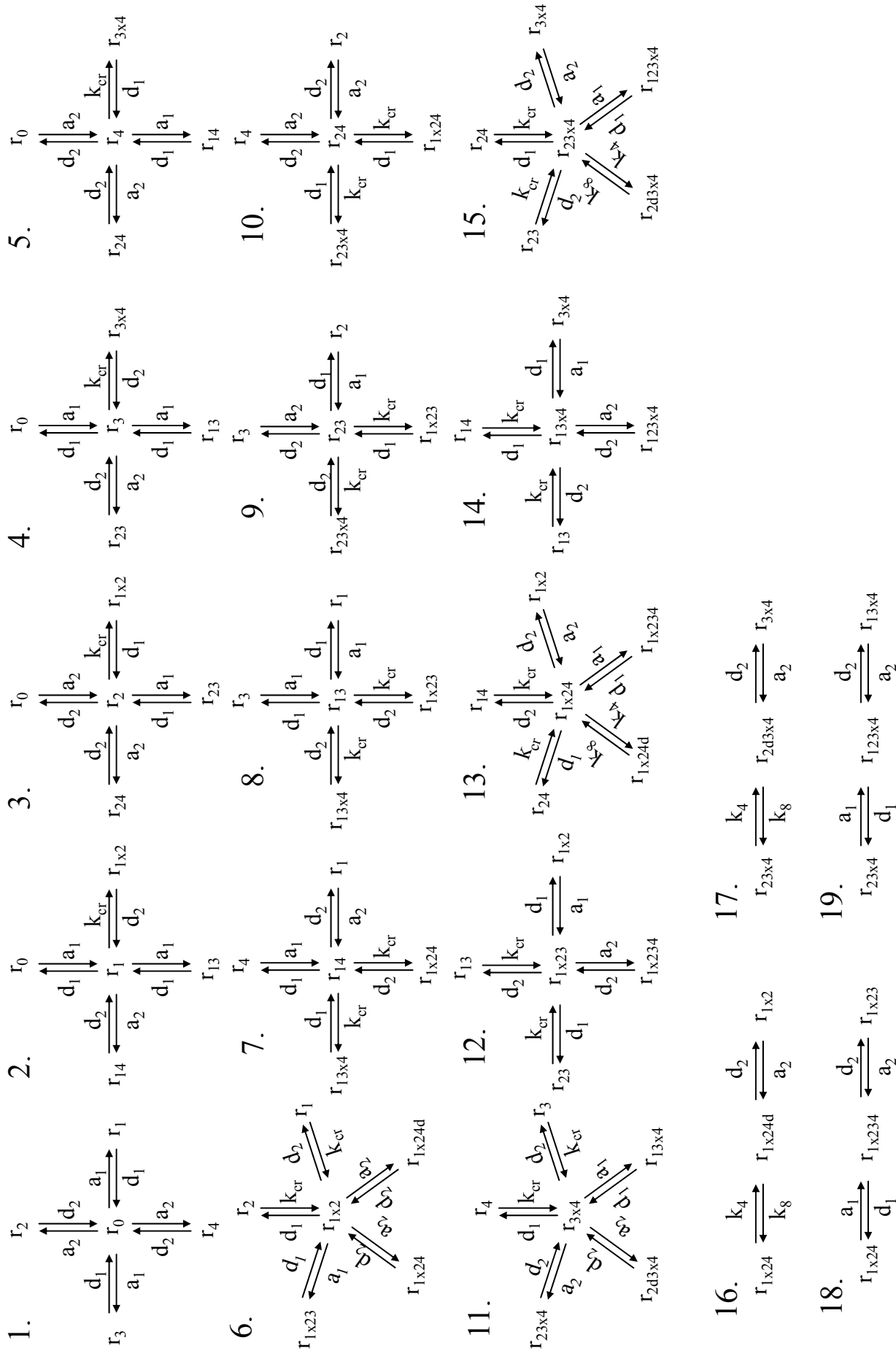
Rules for modelling kinetics of the insulin receptor

Figure S2



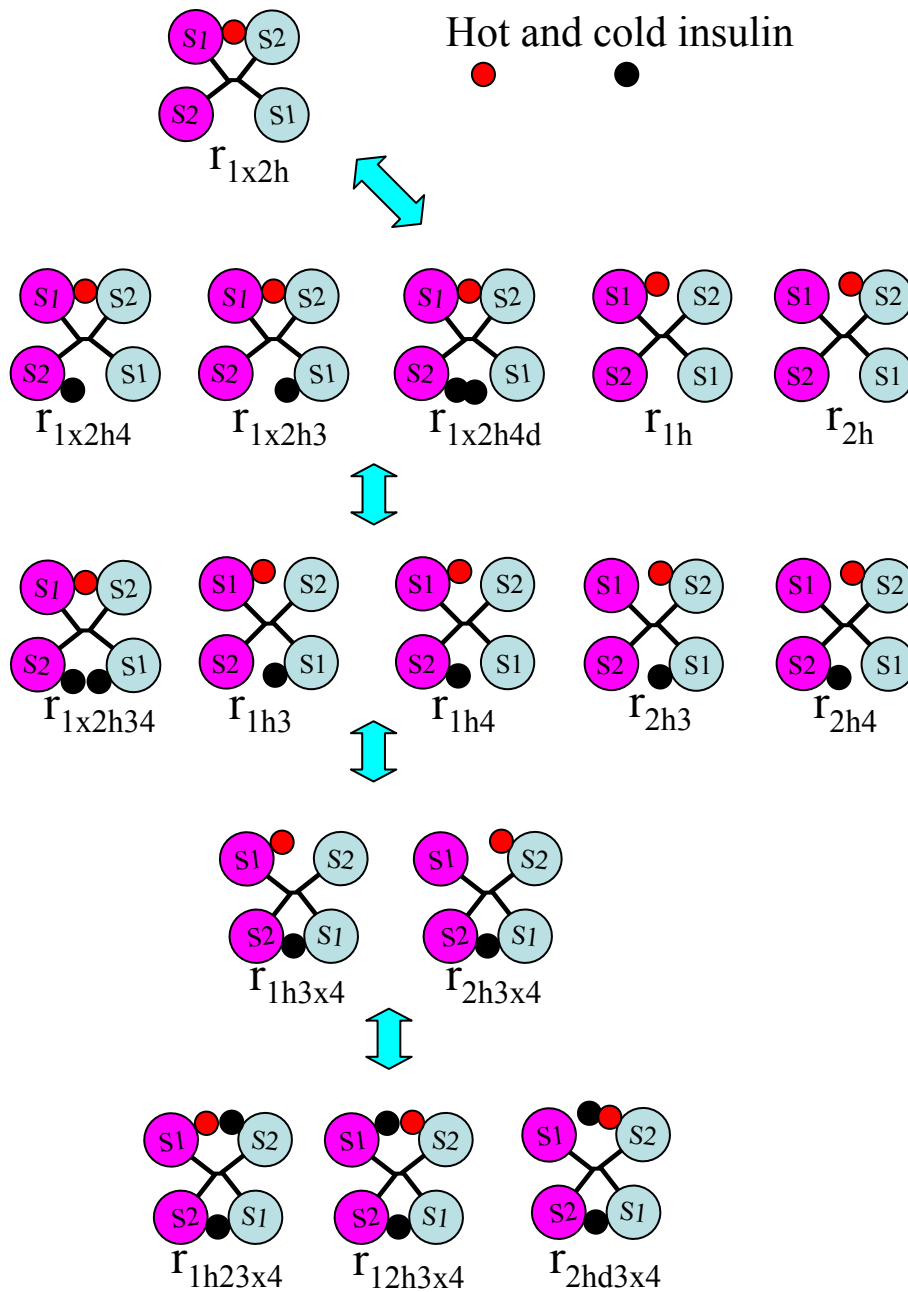
Insulin receptor intermediaries used for modelling insulin binding

Figure S3



Reaction scheme describing interaction of insulin with the insulin receptor. See main text for explanation of the abbreviations.

Figure S4



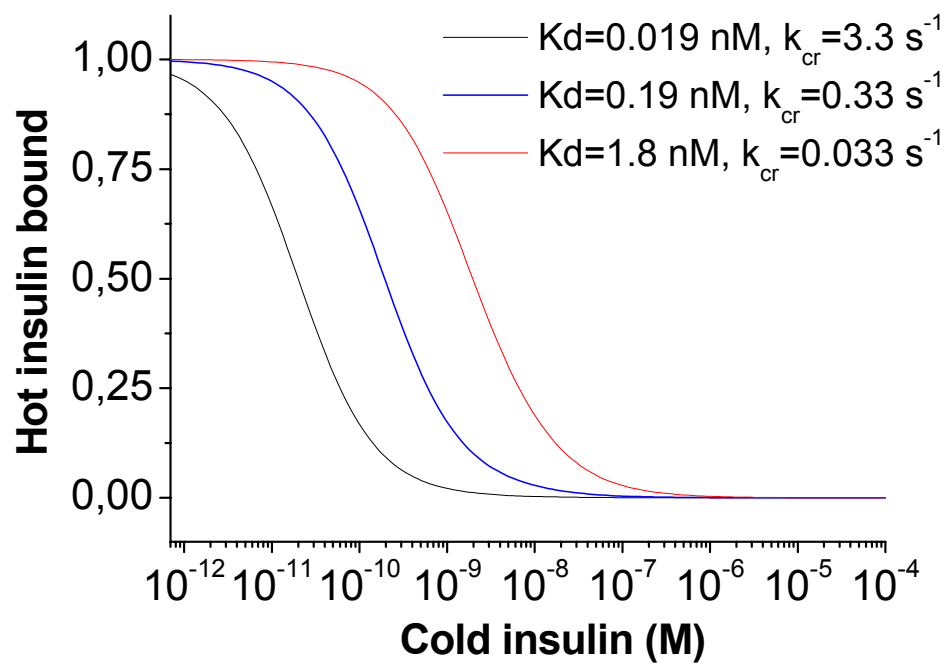
Insulin receptor intermediaries used for modelling the ligand dependence of the receptor dissociation rate

Figure S6

1. $r_0' = -a_1 \cdot r_0 \cdot i_{im} + d_1 \cdot r_1 - a_2 \cdot r_0 \cdot i_m + d_2 \cdot r_4 - a_1 \cdot r_0 \cdot i_m + d_1 \cdot r_3 - a_2 \cdot r_0 \cdot i_m + d_2 \cdot r_2 + k_{ex} \cdot r_{0eyb}$
2. $r_1' = -k_{cr} \cdot r_1 + d_2 \cdot r_{1x2} - a_1 \cdot r_1 \cdot i_{im} + d_1 \cdot r_{13} - a_2 \cdot r_1 \cdot i_{im} + d_2 \cdot r_{14} - d_1 \cdot r_1 + a_1 \cdot r_0 \cdot i_{ms}$
3. $r_2' = -k_{cr} \cdot r_2 + d_1 \cdot r_{1x2} - a_1 \cdot r_2 \cdot i_{im} + d_1 \cdot r_{23} - a_2 \cdot r_2 \cdot i_{im} + d_2 \cdot r_{24} - d_2 \cdot r_2 + a_2 \cdot r_0 \cdot i_{ms}$
4. $r_3' = -k_{cr} \cdot r_3 + d_2 \cdot r_{3x4} - a_1 \cdot r_3 \cdot i_{im} + d_1 \cdot r_{13} - a_2 \cdot r_3 \cdot i_{im} + d_2 \cdot r_{23} - d_1 \cdot r_3 + a_1 \cdot r_0 \cdot i_{ms}$
5. $r_4' = -k_{cr} \cdot r_4 + d_1 \cdot r_{3x4} - a_1 \cdot r_4 \cdot i_{im} + d_1 \cdot r_{14} - a_2 \cdot r_4 \cdot i_{im} + d_2 \cdot r_{24} - d_2 \cdot r_4 + a_2 \cdot r_0 \cdot i_{ms}$
6. $r_{1x2}' = -d_2 \cdot r_{1x2} + k_{cr} \cdot r_1 - a_2 \cdot r_{1x2} \cdot i_d + d_2 \cdot r_{1x24d} - a_2 \cdot r_{1x2} \cdot i_{im} + d_2 \cdot r_{1x24} - a_1 \cdot r_{1x2} \cdot i_{im} + d_1 \cdot r_{1x23} - d_1 \cdot r_{1x2} + k_{cr} \cdot r_2 - k_{end} \cdot r_{1x2}$
7. $r_{14}' = -d_2 \cdot r_{14} + a_2 \cdot r_1 \cdot i_{im} - k_{cr} \cdot r_{14} + d_2 \cdot r_{1x24} - k_{cr} \cdot r_{14} + d_1 \cdot r_{13x4} - d_1 \cdot r_{14} + a_1 \cdot r_4 \cdot i_{ms}$
8. $r_{13}' = -d_1 \cdot r_{13} + a_1 \cdot r_1 \cdot i_{im} - k_{cr} \cdot r_{13} + d_2 \cdot r_{1x23} - k_{cr} \cdot r_{13} + d_2 \cdot r_{13x4} - d_1 \cdot r_{13} + a_1 \cdot r_3 \cdot i_{ms}$
9. $r_{23}' = -d_1 \cdot r_{23} + a_1 \cdot r_2 \cdot i_{im} - k_{cr} \cdot r_{23} + d_1 \cdot r_{1x23} - k_{cr} \cdot r_{23} + d_2 \cdot r_{23x4} - d_2 \cdot r_{23} + a_2 \cdot r_3 \cdot i_{ms}$
10. $r_{24}' = -d_2 \cdot r_{24} + a_2 \cdot r_2 \cdot i_{im} - k_{cr} \cdot r_{24} + d_1 \cdot r_{1x24} - k_{cr} \cdot r_{24} + d_1 \cdot r_{23x4} - d_2 \cdot r_{24} + a_2 \cdot r_4 \cdot i_{ms}$
11. $r_{3x4}' = -d_2 \cdot r_{3x4} + k_{cr} \cdot r_3 - a_1 \cdot r_{3x4} \cdot i_{im} + d_1 \cdot r_{13x4} - a_2 \cdot r_{3x4} \cdot i_d + d_2 \cdot r_{23x4} - a_2 \cdot r_{3x4} \cdot i_{im} + d_2 \cdot r_{23x4} - d_1 \cdot r_{3x4} + k_{cr} \cdot r_4 - k_{end} \cdot r_{3x4}$
12. $r_{1x23}' = -d_1 \cdot r_{1x23} + a_1 \cdot r_{1x2} \cdot i_{im} - a_2 \cdot r_{1x23} \cdot i_{im} + d_2 \cdot r_{1x234} - d_1 \cdot r_{1x23} + k_{cr} \cdot r_{23} - d_2 \cdot r_{1x23} + k_{cr} \cdot r_{13} - k_{end} \cdot r_{1x23}$
13. $r_{1x24}' = -d_2 \cdot r_{1x24} + a_2 \cdot r_{1x2} \cdot i_{im} - a_1 \cdot r_{1x24} \cdot i_{im} + d_1 \cdot r_{1x234} - k_4 \cdot r_{1x24} \cdot i_{im} + k_8 \cdot r_{1x24d} - d_1 \cdot r_{1x24} + k_{cr} \cdot r_{24} - d_2 \cdot r_{1x24} + k_{cr} \cdot r_{14} - k_{end} \cdot r_{1x24}$
14. $r_{13x4}' = -d_1 \cdot r_{13x4} + a_1 \cdot r_{3x4} \cdot i_{im} - a_2 \cdot r_{13x4} \cdot i_{im} + d_2 \cdot r_{123x4} - d_2 \cdot r_{13x4} + k_{cr} \cdot r_{13} - d_1 \cdot r_{13x4} + k_{cr} \cdot r_{14} - k_{end} \cdot r_{13x4}$
15. $r_{23x4}' = -d_2 \cdot r_{23x4} + a_2 \cdot r_{3x4} \cdot i_{im} - a_1 \cdot r_{23x4} \cdot i_{im} + d_1 \cdot r_{123x4} - k_4 \cdot r_{23x4} \cdot i_{im} + k_8 \cdot r_{23x4d} - d_2 \cdot r_{23x4} + k_{cr} \cdot r_{23} - d_1 \cdot r_{23x4} + k_{cr} \cdot r_{24} - k_{end} \cdot r_{23x4}$
16. $r_{1x24d}' = -d_2 \cdot r_{1x24d} + a_2 \cdot r_{1x2} \cdot i_d - k_8 \cdot r_{1x24d} + k_4 \cdot r_{1x24} \cdot i_{im} - k_{end} \cdot r_{1x24d}$
17. $r_{23x4d}' = -d_2 \cdot r_{23x4d} + a_2 \cdot r_{3x4} \cdot i_d - k_8 \cdot r_{23x4d} + k_4 \cdot r_{23x4} \cdot i_{im} - k_{end} \cdot r_{23x4d}$
18. $r_{1x234}' = -d_2 \cdot r_{1x234} + a_2 \cdot r_{1x23} \cdot i_{im} - d_1 \cdot r_{1x234} + a_1 \cdot r_{1x24} \cdot i_{im} - k_{end} \cdot r_{1x234}$
19. $r_{123x4}' = -d_2 \cdot r_{123x4} + a_2 \cdot r_{13x4} \cdot i_{im} - d_1 \cdot r_{123x4} + a_1 \cdot r_{23x4} \cdot i_{im} - k_{end} \cdot r_{123x4}$
20. $r_{0eyt}' = -k_{ex} \cdot r_{0eyt} + k_{end} \cdot r_{1x2} + k_{end} \cdot r_{3x4} + k_{end} \cdot r_{1x23} + k_{end} \cdot r_{1x24} + k_{end} \cdot r_{13x4} + k_{end} \cdot r_{23x4} + k_{end} \cdot r_{1x24d} + k_{end} \cdot r_{23x4d} + k_{end} \cdot r_{1x234} + k_{end} \cdot r_{123x4}$
21. $i_{end}' = -k_{ex} \cdot i_{end} + k_{end} \cdot r_{1x2} + k_{end} \cdot r_{3x4} + 2 \cdot k_{end} \cdot r_{1x23} + 2 \cdot k_{end} \cdot r_{1x24} + 2 \cdot k_{end} \cdot r_{13x4} + 2 \cdot k_{end} \cdot r_{23x4} + 2 \cdot k_{end} \cdot r_{1x24d} + 3 \cdot k_{end} \cdot r_{23x4d} + 3 \cdot k_{end} \cdot r_{1x234} + 3 \cdot k_{end} \cdot r_{123x4}$

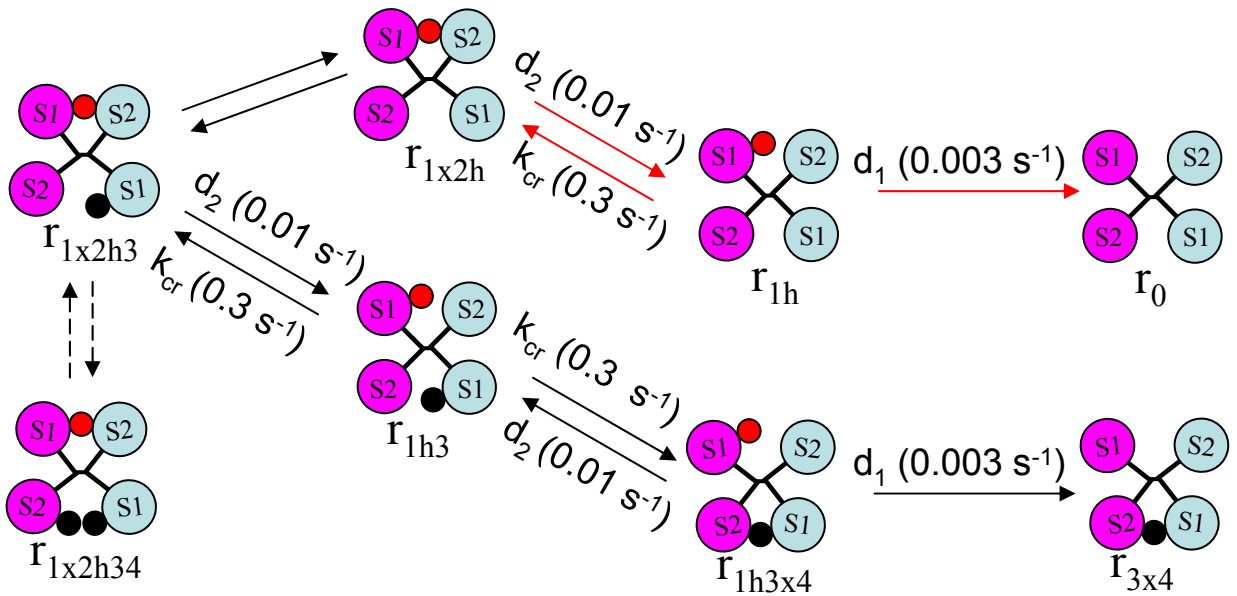
Differential equations corresponding to reactions from Fig. S3 and insulin receptor recycling.

Figure S8



Simulated competition plots of the insulin receptor with various values of the crosslinking constant

Figure S9



Major routes of the insulin receptor dissociation. S1 and S2 stand for site 1 and 2, respectively. Hot insulin is depicted as a red dot, and cold – as black one. The dissociation route in the absence of cold insulin is indicated by red solid lines, in the presence of 100 nM cold insulin – by black solid lines, and the route contributing to the deceleration of the insulin receptor dissociation – by black dashed lines.